Monthly Notices of the ROYAL ASTRONOMICAL SOCIETY

MNRAS **460,** 1417–1427 (2016)
Advance Access publication 2016 May 9

doi:10.1093/mnras/stw1086

Three-body resonance in meteoroid streams

A. Sekhar,[1,2,3]★ D. J. Asher[2] and J. Vaubaillon[4]

[1] *Centre for Earth Evolution and Dynamics, Faculty of Mathematics and Natural Sciences, University of Oslo, Blindern N-0315, Norway*
[2] *Armagh Observatory, College Hill, Armagh BT61 9DG, UK*
[3] *Queen's University of Belfast, University Road, Belfast BT7 1NN, UK*
[4] *IMCCE, Observatoire de Paris, 77 Avenue Denfert Rochereau, F-75014 Paris, France*

Accepted 2016 May 5. Received 2016 May 5; in original form 2015 May 23

ABSTRACT

Mean-motion resonances play an important role in the evolution of various meteoroid streams. Previous works have studied the effects of two-body resonances in different comets and streams. These already established two-body resonances were mainly induced either by Jovian or Saturnian effects but not both at the same time. Some of these resonances have led to spectacular meteor outbursts and storms in the past. In this work, we find a new resonance mechanism involving three bodies – i.e. meteoroid particle, Jupiter and Saturn, in the Perseid meteoroid stream. Long-term three-body resonances are not very common in real small bodies in our Solar system although they can mathematically exist at many resonant sweet spots in an abstract sense in any dynamical system. This particular resonance combination in the Perseid stream is such that it is close to the ratio of 1:4:10 if the orbital periods of Perseid particle, Saturn and Jupiter are considered, respectively. These resonant Perseid meteoroids stay resonant for typically about 2 kyr. Highly compact dust trails due to this unique resonance phenomenon are present in our simulations. Some past and future years are presented where three-body resonant meteoroids of different sizes (or subject to different radiation pressures) are computed to come near the Earth. This is the first theoretical example of an active and stable three-body resonance mechanism in the realm of meteoroid streams.

Key words: celestial mechanics – comets: general – comets: individual: 109P/Swift-Tuttle – meteorites, meteors, meteoroids – planets and satellites: dynamical evolution and stability.

1 INTRODUCTION

The fundamental concept of mean-motion resonances (MMR) in orbital dynamics has been widely explored and studied by different authors. However, correlating real examples in Solar system bodies with theoretical aspects of MMR in celestial mechanics has been a great challenge ever since. To put things into perspective in the context of this work, it is widely known that influences of Jovian MMR in different comets and meteoroid streams (Chambers 1995; Asher & Emel'yanenko 2002; Jenniskens 2006; Ryabova 2006; Vaubaillon, Lamy & Jorda 2006; Soja et al. 2011; Sekhar & Asher 2014) can have a significant impact on their long-term evolution. They play a big role in determining the geometry and evolution of sub-structures in the meteoroid streams. Some of these Jovian MMR have been directly correlated (Asher & Clube 1993; Jenniskens et al. 1998; Arlt et al. 1999; Asher, Bailey & Emel'yanenko 1999; McNaught & Asher 1999; Brown & Arlt 2000; Rendtel 2007; Sato & Watanabe 2007; Christou, Vaubaillon & Withers 2008; Sekhar & Asher 2014) with well-observed meteor outbursts and storms in the past. Such comparisons and future predictions are one of the great applications of orbital studies related to meteor showers. The effects of MMR due to other planets in various meteoroid streams have not been studied at such length like Jovian MMR. Nevertheless there are previous works exploring them in some detail especially the ones related to Saturnian MMR (Brown 1999; Sekhar & Asher 2013) and Uranian MMR (Williams 1997; Brown 1999) in meteoroid streams.

All these examples mentioned above are two-body MMR. In these cases, the individual meteoroid particle gets locked in resonance due to periodic effects from one massive body (i.e. usually a planet). Hence this resonance mechanism involves total of two bodies revolving around the central body (i.e. the Sun). There are plenty of examples, not just meteoroid stream particles, of small bodies getting trapped in two-body MMR in the Solar system. However, real examples of three-body MMR in the Solar system have been rarer; the first well-known example was the Laplacian resonance in the Galilean satellite system (Laplace 1799) involving Ganymede, Europa and Io exhibiting 1:2:4 MMR, respectively. The Laplacian relation has been studied at some length in the past (see Murray & Dermott 1999, section 8.16). After this well-known discovery, a further example of natural satellites getting locked in three-body MMR, namely the Uranian satellites Miranda, Ariel and Umbriel, was apparently identified but ceased to be a real three-body MMR (Murray & Dermott 1999, section 8.16) after better observations

★ E-mail: aswin.sekhar@geo.uio.no

© 2016 The Authors
Published by Oxford University Press on behalf of the Royal Astronomical Society

which eventually led to improved orbital elements. Later work (Nesvorný & Morbidelli 1998; Morbidelli & Nesvorný 1999) showed that three-body MMR plays an important role in the long-term evolution of the asteroid belt. Subsequently Smirnov & Shevchenko (2013) found that there are a large number of asteroids trapped in three-body MMR involving both Jupiter and Saturn. Most recently Gallardo (2014) mapped an atlas of resonant locations feasible for three-body MMR in the Solar system.

Although the topic of three-body MMR led to studies in the case of natural satellites and asteroids in the last few decades, none seems to have explored or made a systematic search for them in the realm of comets and meteoroid streams. In this work, we investigate this problem and show conclusively that three-body MMR, involving Jupiter, Saturn and a meteoroid, can occur in the Perseid stream. Further calculations looking into the evolution of three-body MMR meteoroids show that meteor outbursts or storms on Earth due to this unique resonance mechanism can be correlated in the past and predicted for the future. Perseids are one of the most prolific annual showers (Rendtel 2014) and are well understood to have originated (Jenniskens et al. 1998; Jenniskens 2006) from 109P/Swift-Tuttle which is known to be an active comet.

2 SEPARATION OF THREE-BODY AND TWO-BODY RESONANCES

In Sections 2–4 the MERCURY package (Chambers 1999) incorporating the RADAU algorithm (Everhart 1985) is used for simulating orbits in gravitational *N*-body integrations (Sun + 8 planets). Osculating elements for planets were from JPL Horizons (Giorgini et al. 1996). For 109P they were from Marsden & Williams (2008); cometary non-gravitational parameters are unavailable as Marsden et al. (1993) concluded that 109P's observations back to 69 BC can be fitted gravitationally. Therefore effects like non-gravitational forces, Yarkovsky and YORP are not included for the parent body 109P/Swift-Tuttle.

In this work we focus on true three-body resonances involving Perseid particles with both Jupiter and Saturn. Previous works (Jenniskens et al. 1998; Emel'yanenko 2001) have shown the existence of 1:10, 1:11 and 1:12 Jovian MMR in Perseids. Our test simulations independently indicated the possibility for 1:4 Saturnian MMR (not shown here) as well.

This inspired us to check for a possibility of three-body resonance with triple ratio 1:4S:10J involving both these planets. Saturn and Jupiter are themselves near a 2:5 commensurability (but never in exact resonance) called the 'Great Inequality' (Murray & Dermott 1999, page 10). Counterintuitively, for three-body MMR to exist, it is not necessary that two individual pairs are resonant with each other.

Gallardo (2014) has looked into the abstract cases of three-body resonances in the Solar system and mapped locations (in terms of the 'nominal resonance location' a_n) favourable for such resonances. Circular coplanar orbits are assumed for two planets and the resonance locations can be calculated for test particles with any value of eccentricity e and inclination i. This technique gives an estimation of strengths of resonances and is very useful to compare between different possible three-body MMRs and distinguish between the weakest and strongest MMRs. Hence we use this method here, to find the strongest three-body MMR resonance candidate locations in the Perseid stream.

In terms of mean motions (cf. equation 1 below) the configuration closest to this 1:4S:10J resonance location is 2-1J+2S, for which the semimajor axis a takes the value $a_n = 24.41$ au. Using the code developed by Gallardo (2014), available at www.fisica.edu.uy/~gallardo/atlas, we recalculate all the possible lower order resonances: order of resonance q ≤ 10 for $a = 23$–26 au with degree p ≤ 20 for the nominal $e = 0.95$, $i = 113°$, $\omega = 150°$ of Perseids, these e, i, ω being taken from IAU-MDC (Meteor Data Center). The result yielded 14 MMRs with strengths ranging from 10^{-6} to 10^{-2} out of which two MMRs have significantly higher strengths by an order of magnitude compared to other configurations (Table 1 shows the first six strong candidates, amongst all the 14 MMRs displayed by the code, in descending order of strength). The first and sixth highest strength MMRs (which are discussed in this work) relevant in the case of Perseids are at nominal resonance locations $a_n = 24.41$ au (corresponding resonant configuration 2-1J+2S) and 23.75 au (corresponding resonant configuration 2+1J-3S), respectively. For an approximate estimate of a_n, one can take planetary mean motions considering each individual planet to be on an unperturbed Kepler orbit, and apply Gallardo's equation 2 using masses and mean semimajor axes of Jupiter and Saturn (masses and mean a values may be taken, for example, from Bretagnon 1982).

As discussed in Gallardo's section 2 the actual location of the MMR depends on the precession of perihelia and on all the gravitational effects of the planets. With $a_n = 24.41$ we find ratios of orbital periods $P_m = 4.08 \times P_S = 10.16 \times P_J$ (cf. 1:4S:10J; in terms of 2-1J+2S note that $2 \times 1 - 1 \times 10.16 + 2 \times 4.08 = 0$). Here m, S and J correspond to meteoroid particle, Saturn and Jupiter, respectively. The osculating a of any resonant particle librates, approximately about a_n.

Table 2 gives the resonance locations a_n and order q for the two-body and three-body MMRs discussed in this work. The order of the three-body MMR is $q = |k_0 + k_1 + k_2|$ (k_i as defined in equation

Table 1. Resonant configurations, order of resonances, mean resonance locations and approximate strengths in decreasing order of strength (explained in Gallardo 2014) for different three-body MMR for nominal Perseid orbital elements.

MMR	Order of resonance q	Mean resonance location a_n (au)	Strength $\times 10^{-2}$
2-1J+2S	3	24.41	7.021
6-1J+1S	6	24.19	1.567
8-2J+3S	9	24.24	0.695
14-1J-6S	9	24.03	0.218
10+1J-5S	6	24.01	0.201
2+1J-3S	0	23.75	0.168

Table 2. Mean resonance location and order of resonances for the three-body MMR and nearest two-body MMRs in Perseids. Although the technical nomenclature for this particular three-body MMR in Perseids is 2-1J+2Sand 2+1J-3S, the ratio of orbital periods can be approximated to 1:4S:10J for Perseid particle, Saturn and Jupiter respectively. P denotes the approximate interval (cf. Sekhar & Asher 2013) until the next series of successive encounters of the same resonant cloud with Earth (see Section 3 later), and corresponds to idealized (without other planetary effects) orbital periods.

MMR	Order of resonance q	Mean resonance location a_n (au)	P (yr)
1:4S	3	24.03	118
1:10J	9	24.14	119
1:4S:10J 2-1J+2S	3	24.41	121
1:4S:10J 2+1J-3S	0	23.75	116

1 below). The order of an exterior two-body MMR of configuration p:(p+q) is q. Typically the lower the order of a resonance, the stronger is the resonance mechanism (if the same planet is involved) for low eccentricities. However, for highly eccentric orbits (like the case discussed here) there could be several overlapping higher order resonances with different strengths as shown by Table 1.

As expected, three-body MMR is much more complicated (Yoder & Peale 1981) than two-body MMR and hence one has to be careful while analysing these resonances. Hence it is critical that we do extensive tests to identify a three-body MMR, rigorously eliminating the strongest two-body MMRs closest to the resonance location connected with the particular three-body MMR of our focus.

Our method to confirm three-body MMR in Perseids is to analyse the evolution of critical angle (or resonant argument) σ for given resonances. For a three-body MMR, this is defined by:

$$\sigma = k_0\lambda_0 + k_1\lambda_1 + k_2\lambda_2 - (k_0 + k_1 + k_2)\varpi_0 \quad (1)$$

where k_i are integers, λ_i are mean longitudes and ϖ is longitude of pericentre. Although there are different possible critical angles, this particular one is the principal critical angle because it is associated in the disturbing function with the term factorized with the lowest order power of e (cf. Gallardo 2014). Because Perseids are retrograde, we define $\varpi = \Omega - \omega$ (Saha & Tremaine 1993; Whipple & Shelus 1993) and not $\Omega + \omega$ (ω is argument of pericentre, Ω is longitude of ascending node). The resonance configuration is $k_0 + k_1P_1 + k_2P_2$ if the resonance involves planets P_1 and P_2: we follow this notation throughout. In our work, the resonant particle is a Perseid and the planets are Saturn and Jupiter.

For 2-1J+2S, the critical angle $\sigma = 2\lambda_m - 1\lambda_J + 2\lambda_S - 3\varpi_m$ is plotted versus time. The key logic for verification is: if σ librates versus time and if there is a correlation in the time evolution of semimajor axis with the critical angle, resonance is confirmed. On the other hand, if σ circulates versus time, it rules out that configuration of resonance.

Nesvorný & Morbidelli (1999) presents an analytical theory for three-body MMRs in the Solar system for planar orbits and discusses the estimation of libration amplitudes and libration time-scales. Nesvorný & Morbidelli (1998) has shown that the approach using this critical angle defined above works for orbits with different eccentricities. Hence it is logical to use this critical argument and analysis technique for the cases mentioned above. So the major task is to plot the relevant critical angles for this three-body MMR as functions of time and verify the nature of their evolution.

Fig. 1(a) shows the 2-1J+2S critical angle σ librating continuously for about 3 kyr. To check the presence or absence of the two-body MMRs (cf. Sekhar & Asher 2013) we plot resonant arguments $\sigma_S = \lambda_S - 4\lambda_m + 3\varpi_m$ for 1:4 Saturnian and $\sigma_J = \lambda_J - 10\lambda_m + 9\varpi_m$ for 1:10 Jovian. Fig. 1(b) and (c) shows σ_J and σ_S clearly undergoing outer circulation during the same time frame for the same particle.

Figs 2(a) and (b) shows the libration in semimajor axis and eccentricity corresponding to the same time frame for the same particle shown in Fig. 1. Resonance can be confirmed if there exists a correlation between the librations in the critical angle and the semimajor axis of the particle; this can be seen here. The phase space resonant angle trajectories for 1:10 Jovian and 1:4 Saturnian MMRs were analysed (Murray & Dermott 1999, section 8.9). Figs 3(a) and (b) clearly show outer circulation for the same Perseid particle for 4 kyr. This definitely rules out the existence of both these individual two-body MMRs during the same time frame for the same particle.

The crucial point is to conclusively establish the absence of two-body MMR cases separately. It is well understood that Jupiter and Saturn are not in two-body MMR and hence we have not repeated those calculations explicitly here. The absence of all these three individual pairs undergoing two-body MMRs do not pose any threat to the existence of three-body MMR, as discussed in Greenberg (1975).

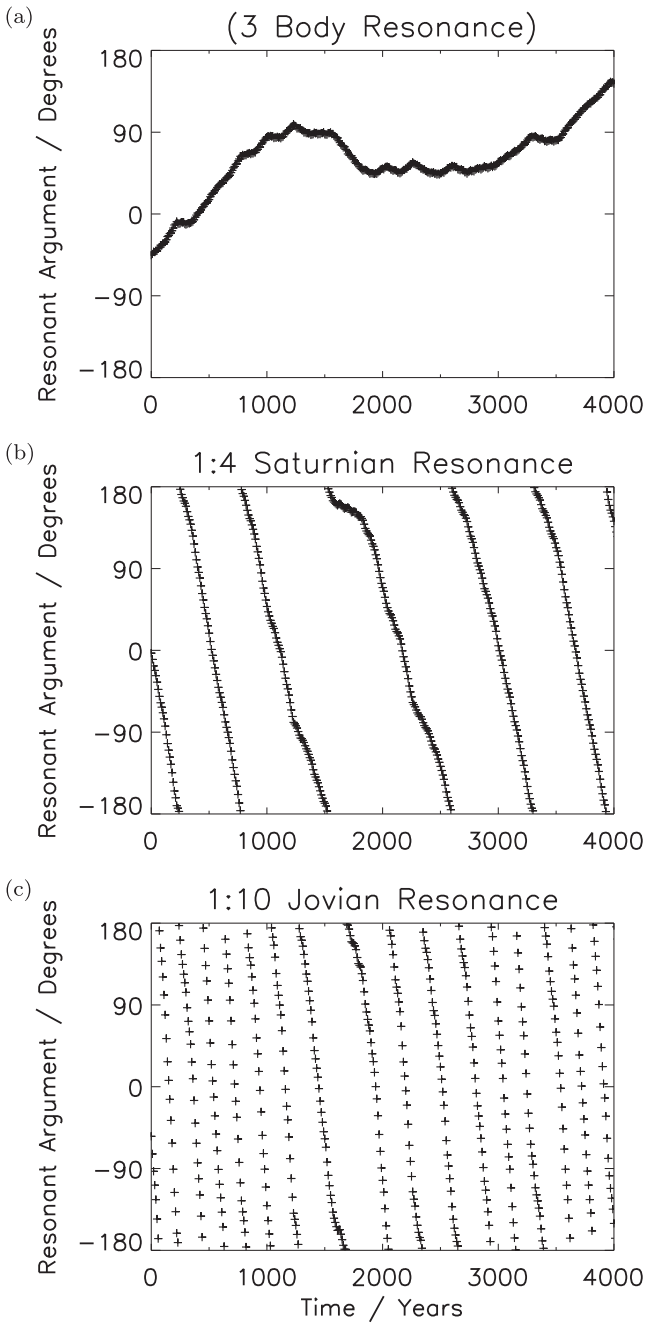

Figure 1. (a) Libration of 2-1J+2S resonant argument for a Perseid test particle (initial $a = 24.334$ au), confirming presence of three-body MMR involving Jupiter and Saturn simultaneously. Outer circulation of (b) 1:10 Jovian (two-body MMR) and (c) 1:4 Saturnian (two-body MMR) resonant arguments for the same particle during same time frame confirm absence of 1:10 Jovian and 1:4 Saturnian separately. Furthermore absence of resonance in (b) and (c) can be directly compared and confirmed with well-defined outer circulation trajectories shown in Figs 3 (a) and (b). Starting epoch (zero time) is JD 1696460.0 = 69 BC August 27.5, the oldest known return of 109P/Swift-Tuttle (Marsden & Williams 2008).

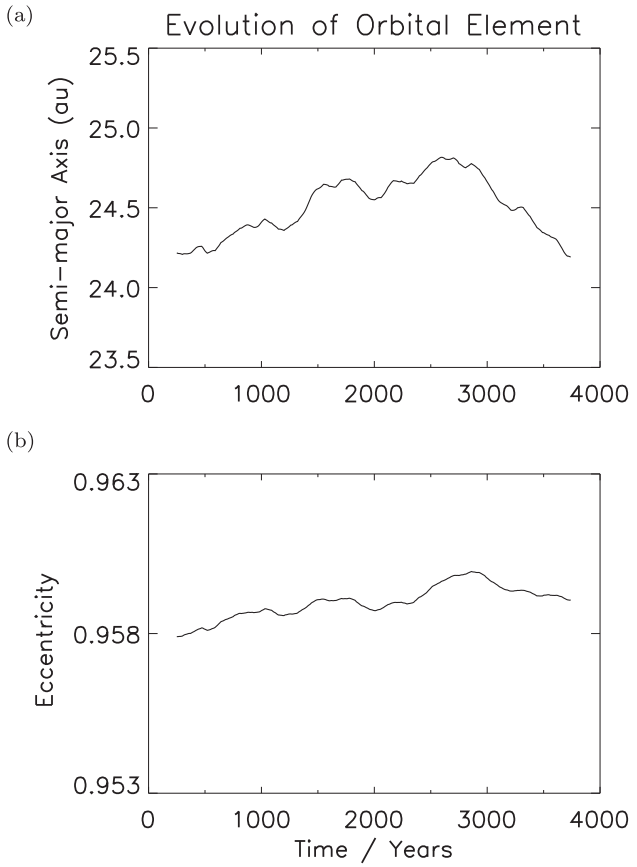

Figure 2. (a) Libration in moving averaged (running window of 500 yr) a matching with libration in 2-1J+2S resonant argument for the same Perseid test particle as in Fig. 1, indicating presence of three-body resonance with Jupiter and Saturn. (b) Evolution of moving averaged (running window of 500 yr) e for the same Perseid test particle as in Fig. 1.

Because our work deals with real comets and meteoroid particles, we did a systematic study to verify the existence of the three-body MMR 2-1J+2S in terms of varying (e, i) orbital space, comparing regions of (e, i) phase space both away from and near the nominal elements of the Perseid stream. Fig. 4 shows the stable regions favouring 2-1J+2S, for trapping particles in resonance. It can be seen that high eccentricity is more favourable for MMRs while low eccentricity and near 90° inclination combinations are least favourable for MMR. It is vital to confirm that the three-body MMR phenomenon does not break down near the real Perseid orbital element phase space and this was the primary motivation for these tests.

3 EXTENT OF RESONANT ZONES

Visualizing the effects of resonance on internal stream structure is important to understand the overall collective behaviour of resonant particles whose individual evolution with time was discussed in Section 2. For this purpose we plot initial semimajor axis a and initial mean anomaly M favouring the three-body MMR mechanism from the starting epoch of 109P/Swift-Tuttle's observed 69 BC return. Fig. 5 shows the geometry of resonant zones for 2-1J+2S libration in the Perseid stream. Two resonant zones can be seen, spanning two different ranges of M. These zones are like potential wells connected with this three-body MMR and particles trapped in these energy points would librate along the boundary of the

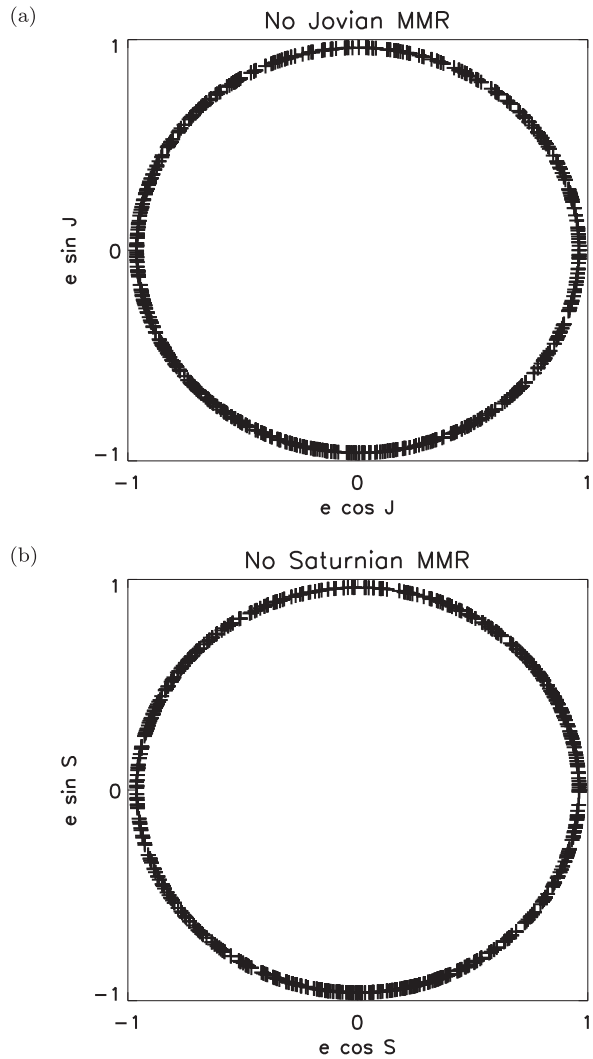

Figure 3. Trajectory phase space for (a) 1:10 Jovian (two-body MMR) and (b) 1:4 Saturnian (two-body MMR) cases for same particle during same time frame show outer circulation and hence confirm absence of either of these resonances over same time frame as shown in Fig. 1. In (b), $J = \sigma_J = \lambda_J - 10\lambda_m + 9\varpi_m$ and in (c), $S = \sigma_S = \lambda_S - 4\lambda_m + 3\varpi_m$.

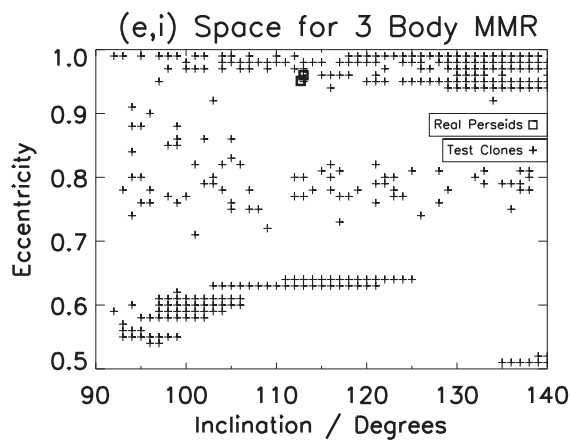

Figure 4. Stable regions of (e, i) space favourable for 2-1J+2S MMR in Perseid-like orbits. The region of this phase space for real Perseids (e, i as given by IAU-MDC) is shown. Points plotted are particles remaining 2-1J+2S resonant (three-body MMR) for 4 kyr from 69 BC perihelion passage.

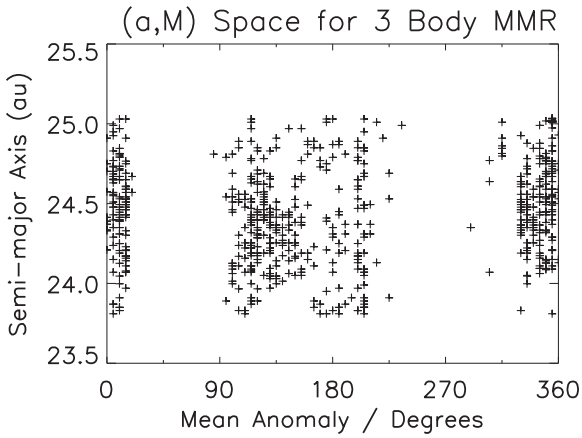

Figure 5. Resonant zones for 2-1J+2S MMR in Perseids in terms of initial a versus initial M. Points plotted are particles remaining 2-1J+2S resonant (three-body MMR) for 4 kyr from 69 BC perihelion passage.

zone trajectories (in case of high-amplitude librations in critical angle σ) or librate very close to the centre of zones (for extremely low-amplitude librations in σ). In a fundamental sense, the motion of particles in resonant potential wells are compared with the behaviour of a simple pendulum (section 8.6, Murray & Dermott 1999). If the particle reaches close to a separatrix, then small effects from gravitational or other forces could disturb the resonance and make the particle circulate (i.e. become non-resonant) over time.

The modus operandi of obtaining this plot involved generating 7200 particles by varying initial a from 23.43 to 25.41 au in steps of 0.02 au, and initial M from 0 to 360° in steps of 5°, keeping q, i, ω, Ω the same as parent body 109P (q = perihelion distance). Particles are integrated 4 kyr and only those trapped continuously in this three-body MMR for 4 kyr are plotted here: for each particle, σ is evaluated for the entire 4 kyr in time steps of 10 yr and a histogram of the resulting σ values is created with bins of 10°. If at least one bin remains void, the particle is flagged as resonant (considering that σ oscillates around some libration centre in such cases). If all bins are populated, the particle is assumed to have circulated through 360° and is flagged as non-resonant. Fig. 5 shows the locations of these resonant particles in (a, M) space at the initial 69 BC epoch.

The picture of resonant zones in this phase space 4 kyr later, or indeed at any different time until 4 kyr, is similar to Fig. 5: at any time there are two zones spanning approximately the same total range in M and a. The central M value of each zone moves progressively forward depending on the orbital period of the MMR; we find it takes about 121 yr to complete one 360° revolution in M.

The orbital period of the parent body during these millennia remains within a few yr of 132 yr (Marsden et al. 1993 table III). Therefore over time the comet drifts backwards through the two resonant zones and can populate both of them with meteoroids, creating clouds of particles in the resonant zones.

P is defined as the time between successive encounters (see Table 2) of Earth with the same resonant cloud (Sekhar & Asher 2014). Previous work (Asher et al. 1999; Emel'yanenko 2001; Sekhar & Asher 2013, 2014) found P ∼ 71 yr for 1:6 Jovian, and P ∼ 88 yr for 1:3 Saturnian in the case of Orionids; P ∼ 33 yr for 5:14 Jovian, and P ∼ 33 yr for 8:9 Saturnian in the case of Leonids.

The trajectory of the comet inside the zones over time may not be uniform and hence different parts of a zone get populated in different intensities and shapes, leading to fine structures inside the zones. These structures would vary greatly depending on ejection conditions (i.e. initial a during each specific perihelion passage and whether this leads to high- or low-amplitude libration in σ), subsequent time evolution and some parts of zones having future close approaches with planets. Predicting an exact intersection leading to a meteor outburst or storm on Earth is directly dependent on whether the Earth traverses through one of these clouds and intersects fine structures or not. Such an intersection would drastically enhance the density of the meteoroid population encountered by Earth or in other words, the Zenithal Hourly Rate (ZHR) could significantly increase during such an event.

Because the gaps between resonant zones are significant (Fig. 5), it is unlikely that Earth would intersect one of the zones on a regular basis every time. But Earth missing these resonant zones does not imply zero meteor activity for Perseids, pointing rather to normal activity without any additional boosting of ZHR due to this particular three-body resonance mechanism. Hence one should be careful not to visualize Earth hitting these discrete clouds as the only reason for substantial Perseid activity on Earth.

Although this represents only a general picture of the potential wells associated with this three-body MMR in space, the simulations show that 2-1J+2S resonant meteoroids can lead to distinct resonant cloud evolutions clearly for many kyr (2 kyr is typical). The range in a spanned by the resonant cloud (Fig. 5) is equivalent to tangential ejection velocities in the range ∼ 4–29 m s^{-1} (approximately 16 m s^{-1} to populate the centre of the zone), directed backward of the comet's heliocentric motion, at the 69 BC return ($a_{\rm comet}$ = 25.41 au) of 109P/Swift-Tuttle. These ejection velocities are realistic in cometary activity (Whipple 1951; Jones 1995; Crifo & Rodionov 1997): the Whipple formula gives 72 m s^{-1} for a particle of diameter 1 mm and Perseid density 2.25 g cm^{-3} (table 2, Babadzhanov & Kokhirova 2009) ejected from a comet nucleus of radius ∼13 km (Lamy et al. 2004) at 109P's perihelion distance in 69 BC. As smaller velocities than this value of 72 m s^{-1} are sufficient to effectively populate this three-body MMR, there is more likelihood of bigger particles getting trapped into resonance, in turn suggesting brighter meteors. Compared to many comets, 109P's relatively large nucleus size favours higher velocity ejections and therefore larger particles ejected at a given velocity. The equivalent particle sizes that have the required range in ejection velocities (again, considering the tangential component only) ∼ 4–29 m s^{-1} are 5–0.6 cm, respectively. The 1737 AD return is similarly favourable in terms of lower ejection velocities, because $a_{\rm comet}$ is lower than at other observed returns, but the positioning in M of the comet relative to the closer of the two resonant zones is not favourable as in 69 BC to populate that resonant zone effectively. All other observed returns require slightly higher ejection velocities to populate resonant locations and indeed no other observed perihelion return except that of 1862 AD is favourable in terms of the position of the comet to populate resonant zones of three-body MMR locations discussed in this work. This is the main reason why the 69 BC return was chosen as the starting epoch here (further discussion in Section 4).

On an independent note, the numerical libration width in a for this three-body MMR from our calculations is about 1.2 au which is in turn close to the semi-analytical libration width of 1.4 au for 1:10 Jovian MMR in Perseids (table 1, Emel'yanenko 2001). This gives greater confidence in our results. Our past work gives a libration width of about 1.2 au (fig. 3, Sekhar & Asher 2014) for 1:6 Jovian MMR in Orionids and 0.1 au (fig. 2.11, Sekhar 2014) for 5:14 Jovian MMR in Leonids which were close to libration widths calculated by Emel'yanenko (2001) of 1.0 au and 0.13 au, respectively. Small differences between analytical and numerical libration widths are normal because the survival times, stability and close encounters

(with planets) of these particles depend on initial conditions and duration of integrations.

4 RESONANT VERSUS NON-RESONANT PARTICLES

In order to check whether three-body MMR causes compact structures in the real Perseid stream, we set up independent integrations to look at the evolution of multiple sets of resonant and non-resonant particles separately and verify the contrast in their dynamics during present times. In the resonant case, 2000 particles were integrated from 109P/Swift-Tuttle's 69 BC return (M = 0-5, 5-10, 350-355, 355-360° at JD 1696460.0; offset chosen by looking at Fig. 5). Initial a varied from 24.434 to 24.634 in steps of 5×10^{-5} au while initial q, i, ω and Ω are kept identical to the parent body. All parameters were the same for the non-resonant particles except the initial mean anomaly was adjusted appropriately (ranges in M = 45–50, 50–55, 260–265, 265–270° at JD 1696460.0; offset chosen by looking at Fig. 5) so that the evolution of multiple sets of non-resonant Perseids can be studied. We verified that no random close encounters with planets significantly affecting the evolution occurred during this offset time and the same number of particles each were always used in both the resonant and non-resonant cases. This is important if we are to compare densities in both evolutions on a like to like basis.

Fig. 6 shows the ecliptic-plane crossings for Perseids in 1993 AD. The contrast in densities between resonant and non-resonant cases (cf. comparisons of libration and circulation regimes in fig. 3 of Emel'yanenko & Bailey 1996) for the same number of particles (2000 clones each) can be clearly seen. This specifically shows the compactness of resonant dust trails in a phase space which primarily deals with the spatial spread near the Earth. Some Perseid particles are seen to directly intersect Earth in 1993 (nodal crossing times for resonant particles were verified to confirm intersecting possibilities at this epoch). The active role of different Jovian and Saturnian two-body MMR in preserving compact dust trails for a long time has previously been demonstrated (Asher et al. 1999; Rendtel 2007; Sato & Watanabe 2007; Sekhar & Asher 2013, 2014). Like these two-body MMR cases, we find that 2-1J+2S MMR (three-body) can produce similar compact structures in the Perseid stream and lead to enhanced meteor activity.

The resonant particles can be seen to occupy only a small part of the entire orbit (close to perihelion and the Earth's orbit) in contrast to non-resonant particles spreading along the whole orbit in Figs 7(a) and (b) for multiple sets of particles from (a,M) phase space. This shows how particles are packed in the along-orbit dimension (in addition to spatial dimensions across ecliptic plane discussed above), with the non-resonant meteoroids dispersed over a large range of heliocentric distances while the resonant particles are concentrated over a small range in heliocentric distances including, at this epoch, the orbit space near the Earth. Since the number of particles is the same and the initial a ranges are the same, between resonant and non-resonant cases, the consistent, significant difference in the distribution in both phase spaces (i.e. ecliptic plane plus along-orbit direction) for multiple sets of resonant and non-resonant particle pairs directly indicates the contrast between the long-term evolution and structure of three-body resonant and non-resonant Perseid meteoroids.

Heliocentric distance r (Fig. 7) does not directly give the exact positions in Cartesian space – i.e. the r value can in principle come from any possible combinations of XYZ coordinates satisfying the Pythagorean expression. Hence it is instructive to double check

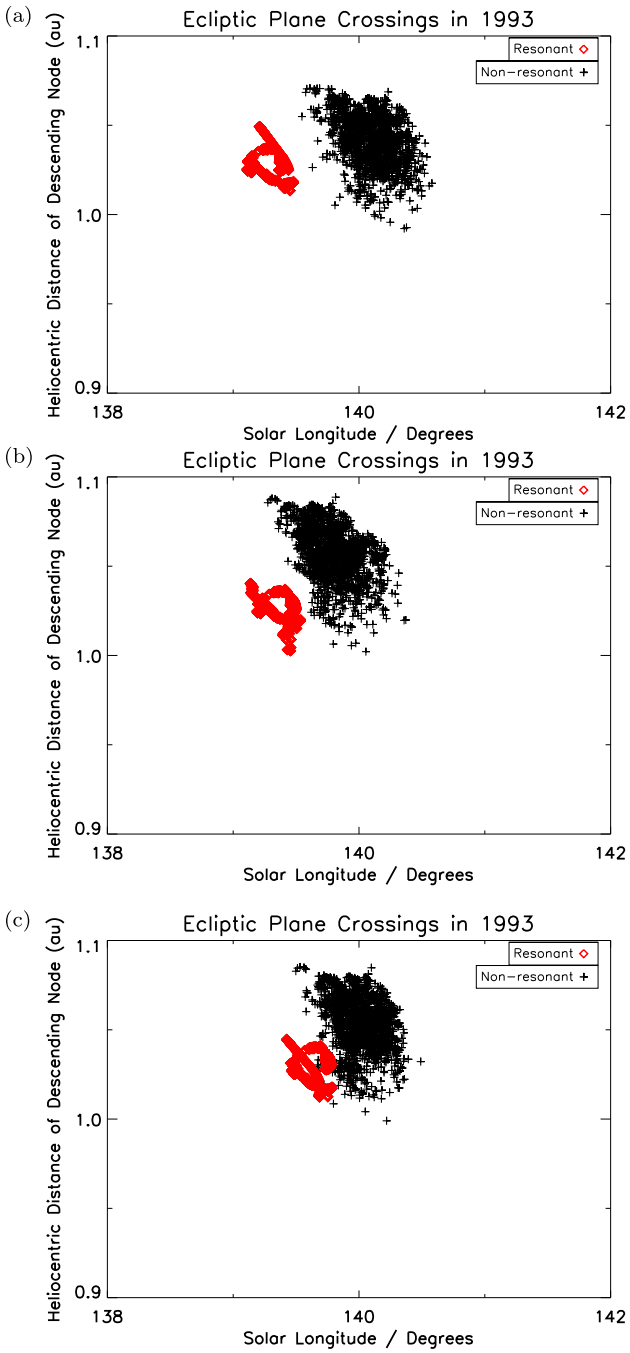

Figure 6. Ecliptic plane crossings of Perseids: heliocentric distance of descending node versus solar longitude (J2000) in 1993 AD, for particles that are 2-1J+2S resonant and non-resonant (circulating in both Jovian and Saturnian two-body MMR and three-body MMR) for particles with different initial ranges in (a) M = 0°–5° (for resonant case) and M = 45°–50° (for non-resonant case) (b) M = 5°–10° (resonant) and M = 50°–55° (non-resonant) (c) M = 350°–355° (resonant) and M = 260°–265° (non-resonant) for subsequent verifications of resonant and non-resonant data sets from Fig. 5. Resonant cases show denser structures whereas significant dispersion can be seen comparatively in the non-resonant meteoroids. Both resonant and non-resonant cases consist of same number (i.e. 2000 clones each) of particles. Integration start time = 69 BC perihelion time of comet 109P.

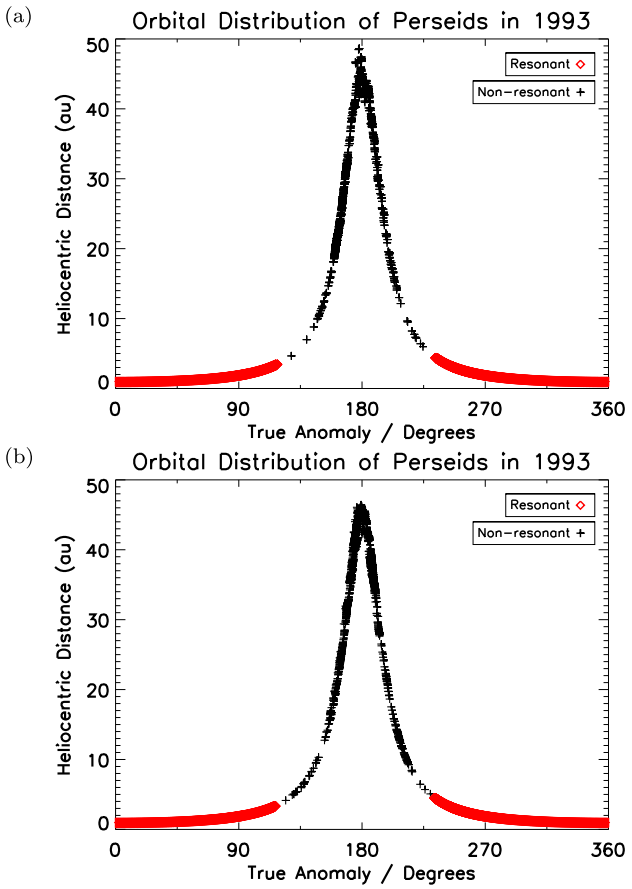

Figure 7. Distribution along the entire orbit – i.e. heliocentric distance versus true anomaly – of Perseid particles for 2-1J+2S case (three-body MMR) and non-resonant Perseids (i.e. neither two-body nor three-body resonant) in 1993 AD (for integrations starting in 69 BC) for different initial ranges in (a) M = 0°–5° (for resonant case) and M = 45°–50° (for non-resonant case) (b) M = 350°–355° (resonant) and M = 260°–265° (non-resonant) for double checking the dynamical differences inferred from Fig. 5. Both resonant and non-resonant cases consist of same number (i.e. 2000 clones each) of particles. The resonant meteoroids show more compactness in the along-orbit dimension compared to the near 360° spread around the entire torus which can be seen in the case of non-resonant meteoroids. Moreover in 1993 a substantial population of the resonant meteoroids come close to the Earth and many are able to intersect Earth which can create enhanced activity.

by explicitly looking at their distribution in XYZ space to ensure all resonant particles remain inside the stream structure. Figs 8(a) and (b) show the XY and XZ space of resonant and non-resonant particles in 3000 AD indicating that the resonant particles stay very much as part of the general Perseid stream orbit into the distant future (for the purpose of meteoroid stream predictions) and no random chaotic effects occur which make them deviate from the typical toroidal meteoroid stream structure. Often a longer time of many 10 kyr or more is required for chaotic effects to dominate in orbital evolution of most small bodies. But because three-body MMR is more closely linked with small stability islands closely surrounded by areas of severe chaotic nature (see fig. 9 in Beaugé et al. 2008), Figs 8(a) and (b) serves as a simple verification to rule out convincingly any random chaotic affects unsettling particles from a typical meteoroid stream torus structure. Ruling out short-term chaos in particle orbits is usually a necessary (but not sufficient) condition for stable resonance.

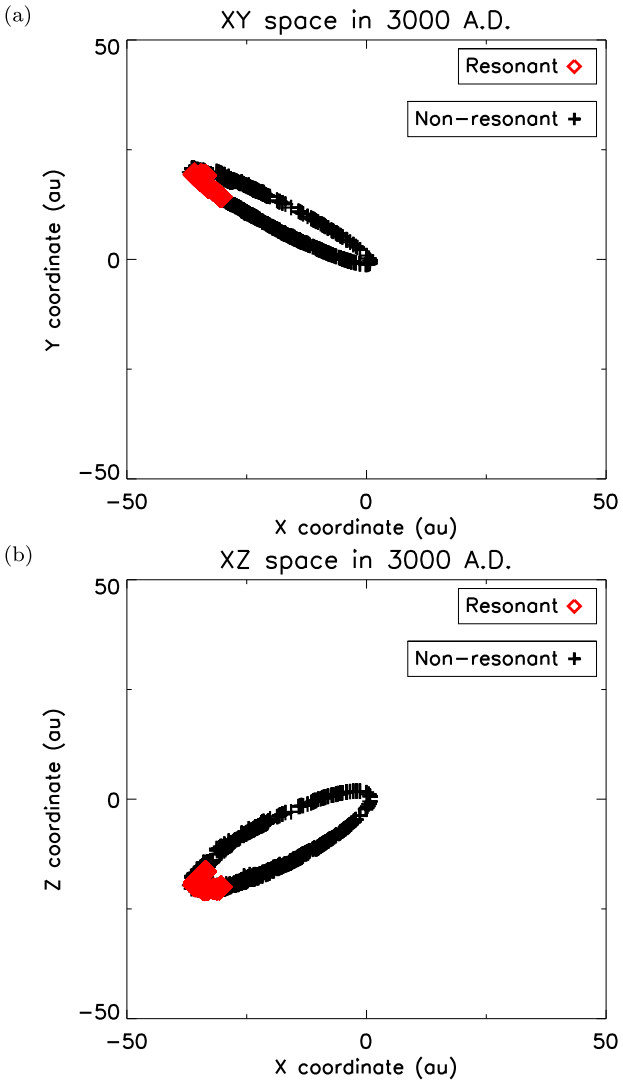

Figure 8. (a) Ecliptic XY space (b) XZ space of Perseid particles for 2-1J+2S case (three-body MMR) and non-resonant Perseids (i.e. neither two-body nor three-body resonant) in 3000 AD (for integrations starting in 69 BC). The plots show that chaotic effects do not disrupt the stream geometry (even though chaos is deeply interconnected with three-body resonances in general compared to two-body resonances) and the resonant meteoroids remain confined to the toroidal structure thus preserving the typical meteoroid stream structure for more than 3 kyr. Both resonant and non-resonant cases consist of same number (i.e. 2000 clones each) of particles.

A systematic check was done to look for the general possibilities of three-body resonant particles coming near the Earth in the recent past and future from all the observed perihelion passages of the parent comet. 100 clones each were ejected at all the observed perihelion passages of the comet (69 BC, 188 AD, 1737 AD, 1862 AD and 1992 AD returns) around each of the six nominal three-body resonant locations in Table 1. Only the 69 BC and 1862 returns are favourable for trapping Perseid particles in strong three-body MMRs: representative particles are plotted in Figs 1, 9–12. And out of all the three-body MMRs in Table 1, the 69 BC return is favourable for both 2-1J+2S and 2+1J-3S configurations. It is found that 1862 AD is favourable for just 2+1J-3S (representative particle in Fig. 11). The other resonant arguments (for configurations listed in Table 1) than the 2-1J+2S and 2+1J-3S do not show libration for starting times corresponding to any of these perihelion passages.

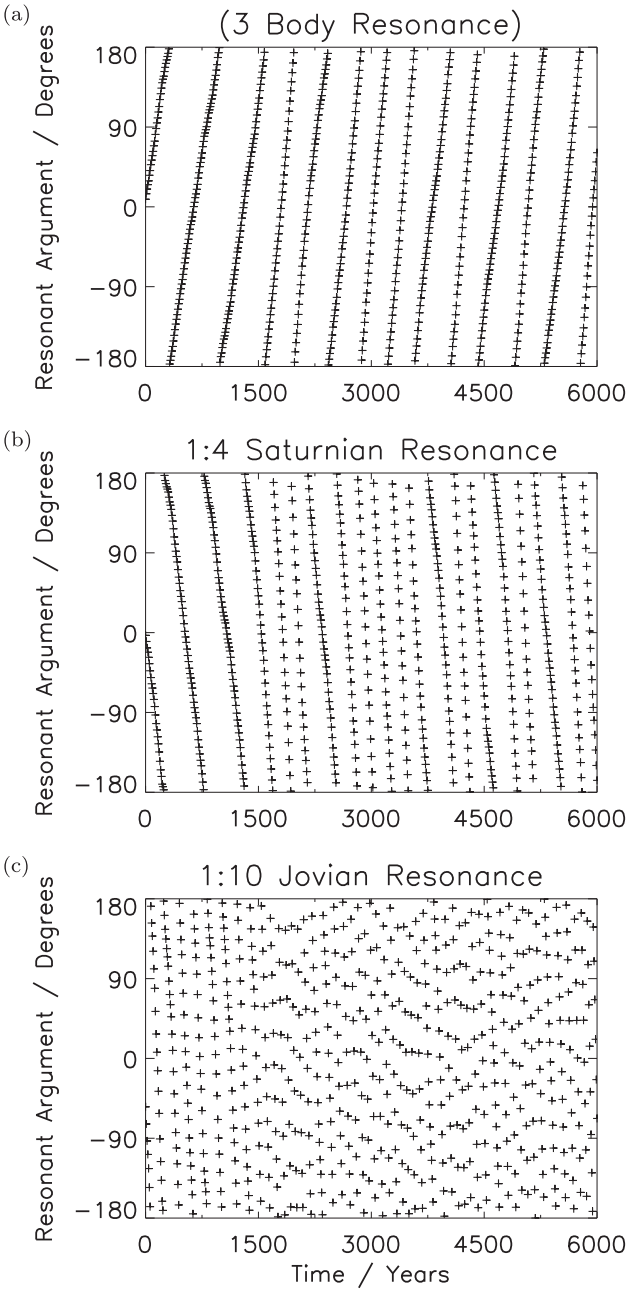

Figure 9. (a) Circulation of 2-1J+2S resonant argument for a Perseid test particle (initial $a = 24.41$ au), confirming absence of three-body MMR involving Jupiter and Saturn simultaneously. Outer circulation of (b) 1:10 Jovian (two-body MMR) and (c) 1:4 Saturnian (two-body MMR) resonant arguments for the same particle during same time frame confirm absence of 1:10 Jovian and 1:4 Saturnian separately. Starting epoch (zero time) is JD 1789915.96 = 188 AD return.

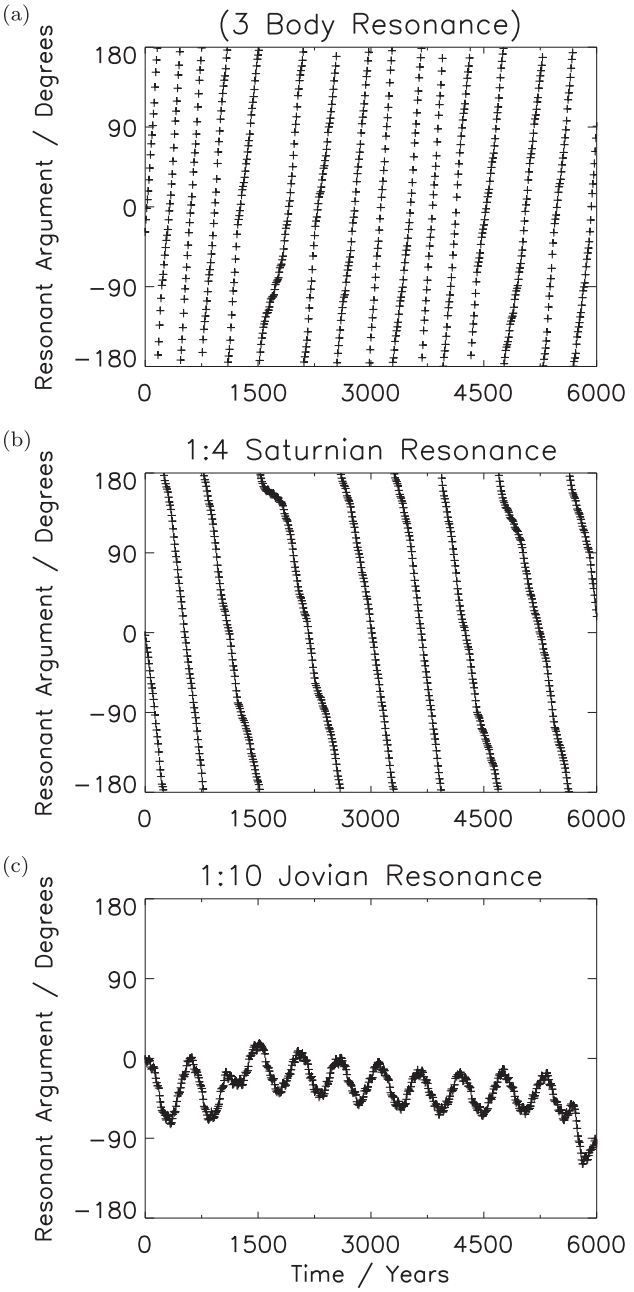

Figure 10. Circulation of (a) 2-1J+2S resonant argument confirming absence of three-body MMR involving Jupiter and Saturn simultaneously and (b) 1:4 Saturnian (two-body MMR) resonant argument showing absence of 1:4 Saturnian for a Perseid test particle (initial $a = 24.41$ au). Small-amplitude libration of (c) 1:10 Jovian (two-body MMR) for the same particle during same time frame confirms presence of strong 1:10 Jovian. Starting epoch (zero time) is JD 2355652.3 = 1737 AD return.

During the remaining observed perihelion returns (188, 1737, 1992), the comet's position is such that either it is mostly efficient to populate 1:10 Jovian MMR (which is the case in 1737 and 1992; representative particles in Figs 10 and 12) or it populates none of the two-body or strong three-body MMRs (representative particle in Fig. 9) discussed in this work.

Thus out of the known observed perihelion returns of the comet, those of 69 BC and 1862 are more favourable for inducing either or both of two distinct three-body MMRs. Hence we integrate two distinct three-body resonant cases (from the two respective perihelion passages) consisting of 2000 particles each (covering the whole a range favouring both these three-body MMR configurations) for 3 kyr forward in time under the influence of four different values of the radiation pressure parameter $\beta = 0$, 0.001, 0.01 and 0.1 (corresponding to different particle sizes). In total therefore, 8 separate integration sets were done to look for possible Earth-meteoroid intersection possibilities.

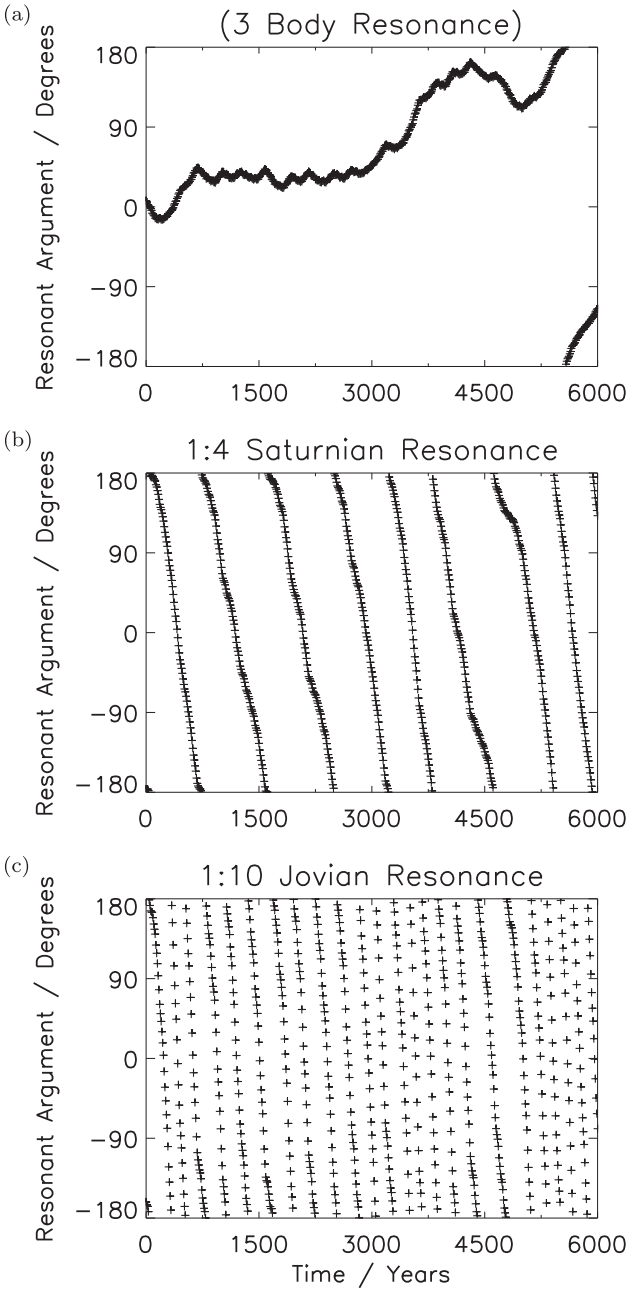

Figure 11. (a) Libration of 2+1J-3S resonant argument for a Perseid test particle (initial $a = 23.40$ au), confirming presence of three-body MMR involving Jupiter and Saturn simultaneously. Outer circulation of (b) 1:10 Jovian (two-body MMR) and (c) 1:4 Saturnian (two-body MMR) resonant arguments for the same particle during same time frame confirm absence of 1:10 Jovian and 1:4 Saturnian separately. Starting epoch (zero time) is JD 2401375.9 = 1862 AD return.

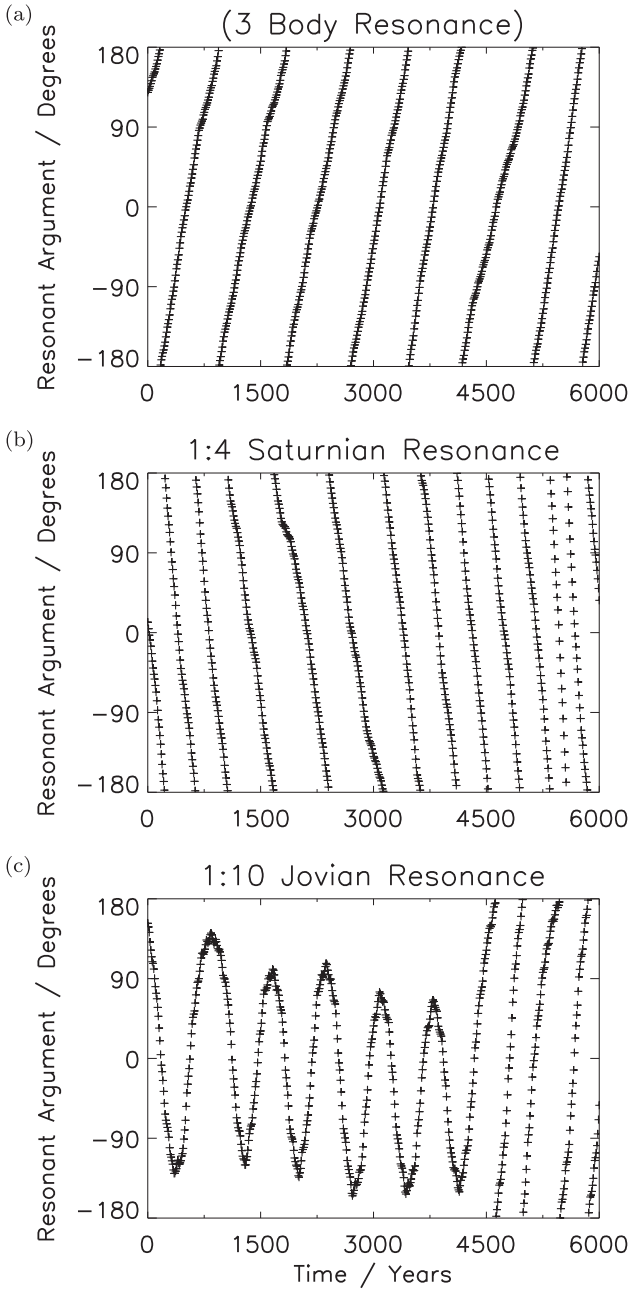

Figure 12. Circulation of (a) 2-1J+2S resonant argument confirming absence of three-body MMR involving Jupiter and Saturn simultaneously and (b) 1:4 Saturnian (two-body MMR) resonant argument showing absence of 1:4 Saturnian for a Perseid test particle (initial $a = 24.41$ au), Libration of (c) 1:10 Jovian (two-body MMR) for the same particle during same time frame confirms presence of 1:10 Jovian. Starting epoch (zero time) is JD 2448968.5 = 1992 AD return, the most recent observed return of 109P/Swift-Tuttle (Marsden & Williams 2008).

Close encounters between three-body resonant particles and Earth were tracked using MERCURY for clones ejected from these two perihelion returns, namely the 69 BC (favouring 2-1J+2S and 2+1J-3S resonance configurations) and 1862 AD (favouring 2+1J-3S) returns. Table 3 shows the close-approach distances between the three-body resonant particles and the Earth for past and future years for different values of β. Sufficient tests (using critical angle and trajectory tests) were done to ensure that the particles listed in Table 3 exhibit three-body resonance (after the incorporation of radiation pressure) and do not show the Jovian and Saturnian two-body resonances during its evolution. The values in the Table show that three-body resonant particles come near the Earth in the past and future time frames thereby indicating the possibilities for enhanced meteor activity from these three-body resonant dust trails. Our integrations show many three-body resonant meteoroids intersecting the Earth in 1992 and 1993. Interestingly Jenniskens et al. (1998) has reported enhanced Perseid activity between 1989 and

Table 3. Close-approach times and minimum close-approach distances between Earth and three-body resonant meteoroids for 69 BC (2-1J+2S resonance) and 1862 AD (2+1J-3S resonance) ejections for different values of radiation pressure β. Cutoff for maximum close-approach distance was set to 1 Hill radius of the Earth.

Ejection epoch	β	Close approach year	Minimum close approach distance (au)
69 BC return (2-1J+2S MMR)	0.0	1297	0.000 45
		1460	0.000 64
		1736	0.000 36
		1880	0.000 68
		1992	0.000 13
		2111	0.000 15
	0.001	1419	0.000 56
		1534	0.000 81
		1764	0.000 98
		1568	0.000 43
		1993	0.000 12
		2108	0.000 10
	0.01	943	0.0090
		1071	0.0091
		1535	0.0059
		1654	0.0071
		1882	0.0097
		2069	0.0057
	0.1	NA	Hyperbolic
1862 AD return (2+1J-3S MMR)	0.0	1984	0.000 30
		2215	0.000 69
		2330	0.000 40
		2446	0.000 21
		2562	0.000 31
		2678	0.000 22
	0.001	1980	0.000 32
		2211	0.000 62
		2442	0.000 63
		2558	0.000 72
		2674	0.000 86
		2790	0.000 65
	0.01	2122	0.0071
		2254	0.0098
		2502	0.0063
		2633	0.0025
		2729	0.0052
		2870	0.0065
	0.1	None	No approach

1996 with peak meteor activity in 1993. It is possible that three-body resonant meteoroids also contributed to the enhanced activity during this period (in addition to two-body Jovian resonances which have been correlated by Jenniskens et al. (1998) previously).

These cases mentioned in Table 3 pertain to three-body resonant particles in a wide range of semimajor axis (covering the entire resonant-zone span) with β values of 0, 0.001, 0.01 and 0.1 ejected tangentially at perihelion, thus giving a general estimate of the nature of their evolution and fate. For extremely accurate meteor density or flux estimations/predictions at precise times, one needs to take multiple sets of particles with finer resolution in semimajor axis, extend the ejection arc (to pre- and post-perihelion points) and include more combinations of β and ejection epochs. This is beyond the scope of this paper but an independent elaborate study is planned for the future. We expect such a detailed study would help us to correlate the specific observed Perseid features between 1989 and 1996 with specific aspects of three-body resonant simulations in an accurate way and come up with more accurate future predictions.

5 CONCLUSION AND FUTURE WORK

We have shown that Perseid particles exhibit a unique three-body resonance mechanism (formal nomenclature of these MMR being 2-1J+2S and 2+1J-3S) close to 1:4:10 MMR involving Perseids, Saturn and Jupiter respectively. Individual particles can get trapped in these resonances for up to ∼4 kyr. Due diligence was followed to ensure that none of these particles show two-body MMR with Jupiter or Saturn separately during the same time frame. Hence it is confirmed that the resonant phenomenon is due to a three-body mechanism rather than the conventional two-body mechanism. Furthermore it is seen that the dust trails can retain very compact structures typically for the order of a few kyr and these compact dust trails can come near the Earth and intersect Earth in past and future times. In summary, this is the first theoretical example of a stable three-body resonance in the realm of meteoroid streams.

We found examples of three-body resonant dust trails intersecting the Earth in 1992 and 1993 which agrees with already observed enhanced Perseid activity between 1989 and 1996 (as reported by Jenniskens et al. 1998). Further work needs to be done to correlate the exact observed features with simulations and give accurate predictions for the future. The future challenge is to run detailed simulations, using finer resolution in the a of ejected particles and extending the ejection arc to pre- and post-perihelion intervals, in order to find precise meteoroid-Earth intersection times and estimate the density or flux of peak meteor activity and the duration of possible enhanced activity due to these three-body MMRs from the already identified favourable perihelion passages.

Because the three-body resonance mechanism also favours clustering and increase of density of meteoroids in space just like in the case of two-body resonances, one can expect spectacular meteor outbursts and storms on Earth from this resonance mechanism in the future. Any prediction for such a future outburst or storm in the near future will be of great theoretical as well as observational value. Further work is planned in this direction so that professional and amateur observers can be alerted and scientific observing campaigns can be launched soon.

ACKNOWLEDGEMENTS

AS acknowledges the Crater Clock project (235058/F20) based at CEED funded through the Centres of Excellence scheme (project number 223272) by the Research Council of Norway and thanks the support from project PI Dr Stephanie Werner. AS and DJA thank the Department of Culture, Arts and Leisure of Northern Ireland for funding astronomical research at Armagh Observatory. We are grateful to Tabaré Gallardo and an anonymous reviewer for thorough and helpful comments and acknowledge the valuable contribution of Dr Gallardo to the research community in making available his software to compute locations and strengths of three-body resonances.

REFERENCES

Arlt R., Rendtel J., Brown P., Velkov V., Hocking W. K., Jones J., 1999, MNRAS, 308, 887
Asher D. J., Clube S. V. M., 1993, QJRAS, 34, 481
Asher D. J., Emel'yanenko V. V., 2002, MNRAS, 331, 126
Asher D. J., Bailey M. E., Emel'yanenko V. V., 1999, MNRAS, 304, L53

Babadzhanov P. B., Kokhirova G. I., 2009, A&A, 495, 353
Beaugé C., Giuppone C. A., Ferraz-Mello S., Michtchenko T. A., 2008, MNRAS, 385, 2151
Bretagnon P., 1982, A&A, 114, 278
Brown P., 1999, PhD thesis, Univ. Western Ontario
Brown P., Arlt R., 2000, MNRAS, 319, 419
Chambers J. E., 1995, Icarus, 114, 372
Chambers J. E., 1999, MNRAS, 304, 793
Christou A. A., Vaubaillon J., Withers P., 2008, Earth Moon Planets, 102, 125
Crifo J. F., Rodionov A. V., 1997, Icarus, 127, 319
Emel'yanenko V. V., 2001, in Warmbein B., ed., ESA SP-495: Proceedings of the Meteoroids . ESA, Noordwijk, p. 43
Emel'yanenko V. V., Bailey M. E., 1996, in Gustafson B. A. S., Hanner M. S., eds, ASP Conf. Ser. Vol. 104, Physics, Chemistry, and Dynamics of Interplanetary Dust. Astron. Soc. Pac., San Francisco, p. 121
Everhart E., 1985, in Carusi A., Valsecchi G. B., eds, Astrophysics and Space Science Library, Vol. 115, Dynamics of Comets: Their Origin and Evolution. Reidel, Dordrecht, p. 185
Gallardo T., 2014, Icarus, 231, 273
Giorgini J. D. et al., 1996, BAAS, 28, 1158
Greenberg R., 1975, MNRAS, 173, 121
Jenniskens P., 2006, Meteor Showers and their Parent Comets. Cambridge Univ. Press, Cambridge
Jenniskens P. et al., 1998, MNRAS, 301, 941
Jones J., 1995, MNRAS, 275, 773
Lamy P. L., Toth I., Fernández Y. R., Weaver H. A., 2004, in Festou M. C., Keller H. U., Weaver H. A., eds, Comets II. Univ. Arizona Press, Tucson, p. 223
Laplace P. S., 1799, Mécanique Céleste by the Marquis de Laplace.
McNaught R. H., Asher D. J., 1999, WGN (J. Int. Meteor Organ.), 27, 85
Marsden B. G., Williams G. V., 2008, Catalogue of Cometary Orbits, 17th edn. Minor Planet Center/Central Bureau for Astronomical Telegrams, Cambridge, MA
Marsden B. G., Williams G. V., Kronk G. W., Waddington W. G., 1993, Icarus, 105, 420
Morbidelli A., Nesvorný D., 1999, Icarus, 139, 295
Murray C. D., Dermott S. F., 1999, Solar System Dynamics. Cambridge Univ. Press, Cambridge
Nesvorný D., Morbidelli A., 1998, AJ, 116, 3029
Nesvorný D., Morbidelli A., 1999, Celest. Mech. Dyn. Astron., 71, 243
Rendtel J., 2007, WGN (J. Int. Meteor Organ.), 35, 41
Rendtel J., ed., 2014, Meteor Shower Workbook 2014. Internat. Meteor Org., Potsdam
Ryabova G. O., 2006, in Lazzaro D., Ferraz-Mello S., Fernández J. A., eds, Proc. IAU Symp. 229, Asteroids, Comets, Meteors. Cambridge Univ. Press, Cambridge, p. 229
Saha P., Tremaine S., 1993, Icarus, 106, 549
Sato M., Watanabe J., 2007, PASJ, 59, L21
Sekhar A., 2014, PhD thesis, Queen's Univ. Belfast
Sekhar A., Asher D. J., 2013, MNRAS, 433, L84
Sekhar A., Asher D. J., 2014, Meteorit. Planet. Sci., 49, 52
Smirnov E. A., Shevchenko I. I., 2013, Icarus, 222, 220
Soja R. H., Baggaley W. J., Brown P., Hamilton D. P., 2011, MNRAS, 414, 1059
Vaubaillon J., Lamy P., Jorda L., 2006, MNRAS, 370, 1841
Whipple F. L., 1951, ApJ, 113, 464
Whipple A. L., Shelus P. J., 1993, Icarus, 101, 265
Williams I. P., 1997, MNRAS, 292, L37
Yoder C. F., Peale S. J., 1981, Icarus, 47, 1

This paper has been typeset from a TEX/LATEX file prepared by the author.